ELSEVIER

Ceramics International 28 (2002) 609–615

CERAMICS INTERNATIONAL

www.elsevier.com/locate/ceramint

Synthesis and properties of sol–gel SBT powder and film

W. Wang*, D.C. Jia, Y. Zhou, J.C. Rao, F. Ye

Department of Materials Science and Engineering, Harbin Institute of Technology, PO Box 433, Harbin 150001, PR China

Received 26 September 2001; received in revised form 14 October 2001; accepted 16 November 2001

Abstract

Nanocrystalline powder with particle size 50 nm and thin film with thickness 2 μm of $SrBi_2Ta_2O_9$ (SBT) were successfully prepared by the sol–gel method, using strontium acetate semihydrate [$Sr(CH_3COO)_2{\cdot}1/2H_2O$] and bismth subnitrate [$BiO(NO_3)$], and tantalum ethoxide [$Ta(OCH_2CH_3)_5$] as source materials, glacial acetic and ethylene glycol as solvents. The XRD and TEM results indicated that SBT layer-perovskite phase powder obtained has to be single phase, Pt layer had a (100) predominate orientation, and the (115), (200) of SBT thin film formed after being annealed at 800 °C for 1 min. The typical hysteresis loop of SBT thin film on $Pt/Ti/SiO_2/Si$ was obtained, and the measured *Pr* and *Ps* values of the SBT thin film were 5.5 and 8.8 $\mu C/cm^2$, respectively.

Keywords: A. Sol–gel technique; C. Ferroelectric properties; $SrBi_2Ta_2O_9$; Thin film

1. Introduction

Ferroelectric films have attracted much attention due to their potential applications in electronic devices such as pyroelectric infrared detectors, optical switches, actuators, dynamic random access memories (DRAMS) [1], and non-volatile random access memories (NVRAMS). Recently, there is interest in the study of bismuth layer structured ferroelectric materials for memory applications. In particular, strontium bismuth tantanate (SBT), one of the bismuth layer structured compounds, is a promising candidate for ferroelectric random access memories (FRAMS) as it shows very little fatigue after 10^{12} cycles under polarization switching [2]. These compounds are called Aurivillius phases and have the general formula of $(Bi_2O_2)^{2+}(A_{m-1}B_mO_{3m+1})^{2-}$, where A and B represent ions with suitable valences and ionic radii (such as Bi, Pb, Ba, Sr, Ca and K for the A site and Ti, Nb, Ta, W, Mo, Fe and Cr for the B site, respectively). A pseudo-perovskite layer ($A_{m-1}BmO_{3m+1}$) is sandwiched between the fuorite type sheets $(Bi_2O_2)^{2+}$, where *m* and *m*-1 are the numbers of oxygen octahedrals and pseudo-perovskite units in a layer, respectively. The lattice structure of SBT, consisting of perovskite (TaO_6) octahedral separated at intervals by bismuth oxide $(Bi_2O_2)^{2+}$ planes, has a spontaneous polarization along its a or b axis. Hence, SBT has a 180° ferroelectric domain configuration and this may be the reason for the good fatigue properties.

Bi layer structured films (e.g. $SrBi_2Ta_2O_9$, $SrBi_2Nb_2O_9$) can be prepared by pulsed laser deposition [3], metal organic chemical vapor deposition [4], metal organic decomposition [5] and the sol–gel method. There are many reports on the sol–gel method in a broad sense [6–8]. The sol–gel process offers many advantages over conventional methods, such as high purity, molecular homogeneity, low-temperature processing, convenient fabrication procedures, and easy control of stoichiometry. However, as starting materials, alkoxides would make the whole fabricating process more susceptible to temperature and ambient humidity, and must be handled under inert atmosphere. Therefore, the alkoxides of some metals such as Ta and Bi were coordinated using pyridine [9], alcohol-amine [10] and acetylacetone [11], and the metal complex compound became stable. But the addition of a complex agent makes it difficult for the control of the processes of gel polymerization. In order to overcome these problems, new raw materials and solvents are used, thus a stable SBT precursor solution can be prepared to allow their handling in air, which makes the operation more convenient.

In this paper, an SBT precursor was fabricated via inorganic materials instead of alkoxides in a solo alkoxide

* Corresponding author. Fax: +86-451-6413922.
E-mail address: ce921@hope.hit.edu.cn (W. Wang).

0272-8842/02/$22.00
PII: S0272-8842(02)00016-0

system. The synthesis of the SBT powder and films by a sol–gel process and the measurements of the microstructure and properties of these materials were reported.

2. Experimental procedures

SBT precursor solutions were synthesized using strontium acetate semihydrate [$Sr(CH_3COO)_2 \cdot 1/2H_2O$, purity 99.9%, Shanghai Chemical Reagent Corporation] and bismth subnitrate [$BiO(NO_3)$, purity 99.9%, Shanghai Kechang Chemical Reagent Corporation], and tantalum ethoxide [$Ta(OCH_2CH_3)_5$, self-made, concentration (261.6 mg/ml) was detected using inductively coupled plasma(ICP)] as source material. Glacial acetic and ethylene glycol were selected as solvents. Strontium acetate and bismuth subnitrate were initially dissolved in glacial acetic acid, tantalum ethoxide mixed with ethylene glycol was added dropwise to the above solution with constant stirring, then the solution was controlled by varying the ethylene glycol content. Addition of 2-methoxyethanol also improved the wetness and uniformity of the coating on the substrate. The resulting concentration of the solutions was 0.1 mol/l. The precursor solutions were spin-coated on $Pt/Ti/SiO_2/Si$ by a spinner operating at a speed of 3000 rpm/min for 60 s. After the coating process, the films were kept in air for 1 h to form gel films by the hydrolysis and polymerization. They were then slowly heated at a rate of 5 °C/min to a baking temperature of 350 °C for the decomposition of residual organics, and finally cooled to room temperature. The above process of coating and baking was repeated several times to increase the thickness of the films. The deposition conditions were same for all samples.

As-prefired films were amorphous in nature. Annealing at a higher temperature was needed to convert the amorphous structure into a crystalline structure. Fig. 1 shows the preparation procedure for the formation of SBT thin films.

Differential scanning calorimetry and thermogravimetric analysis (DSC–TGA; Netzsch-sta449C) were conducted with the heating rate of 10 °C/min to examine the thermal reactions of the gel. The phase of the powder and thin films was examined by X-ray diffraction (XRD, Rigaku Rotaflex D/max-II B) using a scanning speed of 10°/min, an acceleration voltage of 40 kV

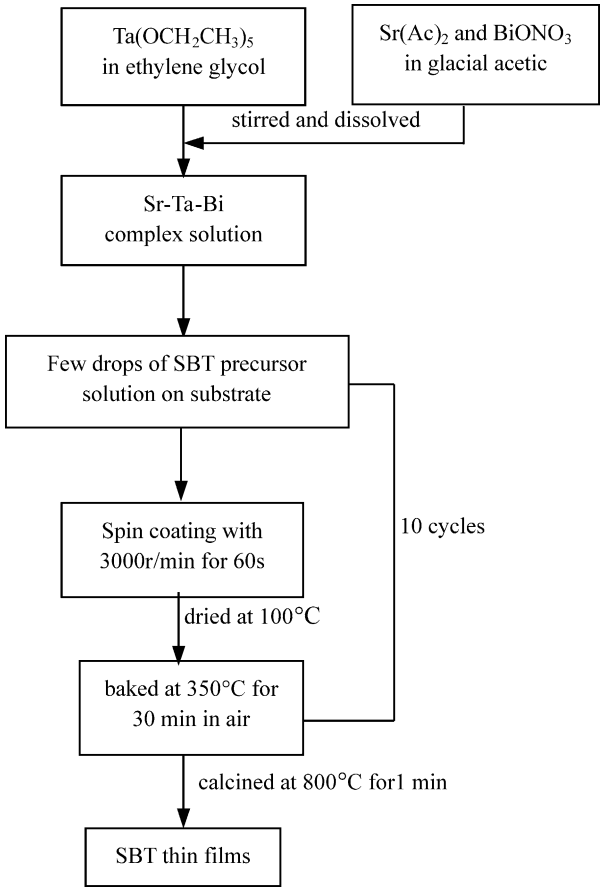

Fig. 1. Flow diagram for the preparation procedure of the SBT thin films.

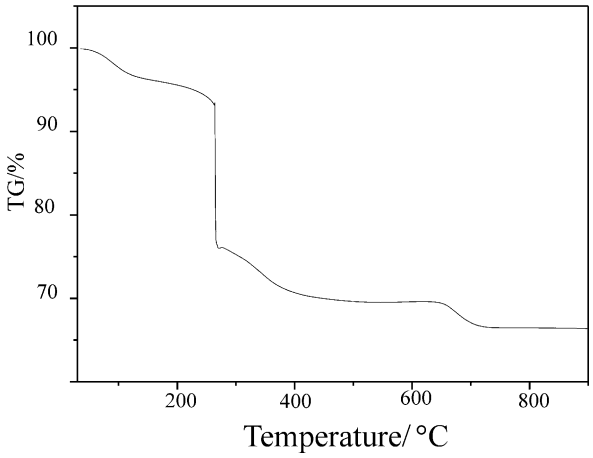

Fig. 2. TG curve of the gel.

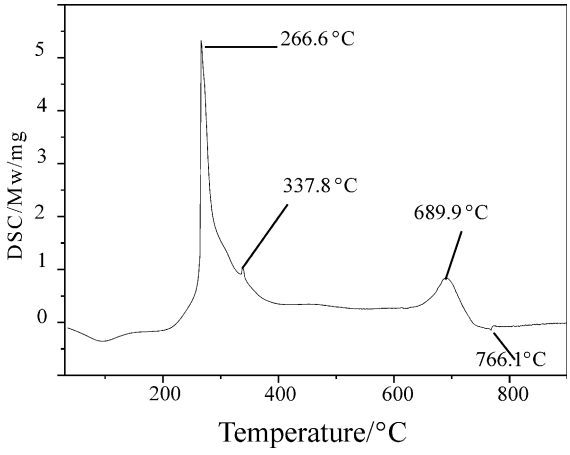

Fig. 3. DSC curve of the gel.

and an electric current of 50 mA. To check the chemical state of the element, X-ray photoelectron spectroscopy (XPS) featuring a hemispherical electron energy analyzer was used. The morphology and the thickness of the deposited films were determined using a scanning electron microscope (SEM). The composition of the SBT films was determined by electron probe microanalysis (EPMA). Morphorlogy of the SBT powder and micro area diffraction of the SBT thin films was examined by transmission electron microscopy (TEM; Philips CM-12) with an acceleration voltage of 120 kV, SBT powder was deconglomerated using ultrasonic vibration in acetone solvent for 1 h. Hysteresis (P–E) loop measurement was performed using a Radiant Technology RT 66A ferroelectric test system.

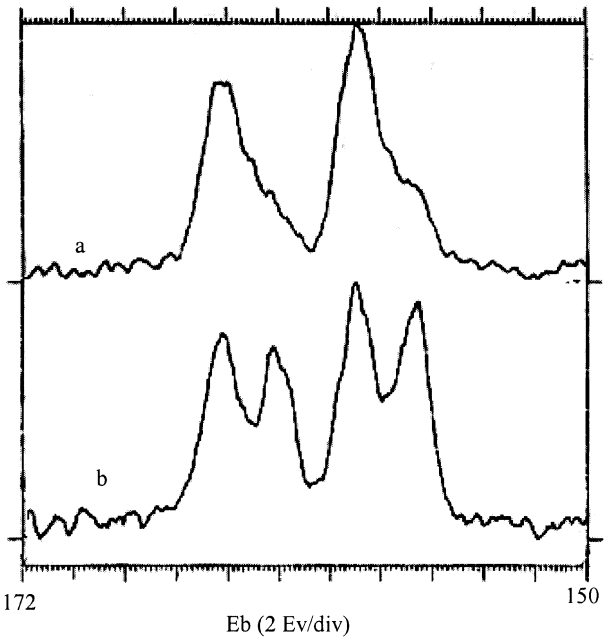

Fig. 4. XPS signal of valence of bismuth (a) the SBT surface; (b) the interface between SBT and platinum.

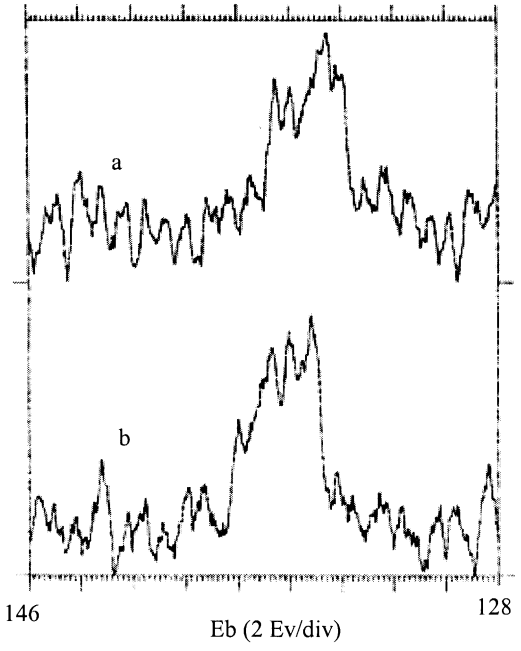

Fig. 5. XPS signal of valence of strontium (a) the SBT surface; (b) the interface between SBT and platinum.

3. Results

3.1. TGA and DTA analysis

Figs. 2 and 3 show the TGA and DSC curves of the gel obtained from solution with a mol ratio of strontium:bismuth:tantalum = 1:2:2. The DSC of the gel revealed two endothermic at 100 and 766.1 °C, and three exothermic peaks at 266.6, 337.8 and 689.9 °C. The first endothermic peak is due to the volatilization of organic compound (such as $HOCH_2CH_2OH$ and n-$C_2H_5ONO_2$), and the weight loss is about 7%; the second small endothermic peak at 766.1 °C is relevant to the crystallization of the SBT powder. Exothermic peaks at 266.6 and 337.8 °C are due to the combustion of many ethoxy groups and a few acetate groups in the

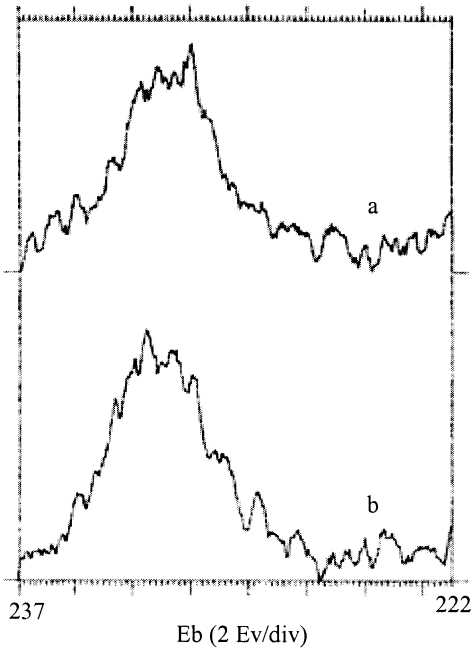

Fig. 6. XPS signal of valence of tantalum (a) the SBT surface; (b) the interface between SBT and platinum.

Table 1
The binding energies of the SBT thin film

Element	Energy level		Valence state	Binding energy(eV)	
Bi	4f7/2	4f5/2	+3	158.8	164.2
Ta	4d	–	+5	231	–
Sr	3d5/2	3d3/2	+2	133.1	135.6

oligomer. These two kinds of organic groups have different rates of weight loss. Weight loss of many ethoxy groups is 17.41% from 250 to 270 °C, and weight loss of a few acetate groups is 6% from 270 to 450 °C. The weight loss of 3% during the temperature range of 600–750 °C indicates combustion of carbon in the framework.

3.2. Spectroscopy

Fig. 4a and b show the change of valence of bismuth at the surface and the interface between SBT and platinum. Obviously, the signal from the film surface is different from that interface. The XPS spectra of the Bi4f peak of the SBT thin film was composed of several doublets which may be due to the various oxidation states as previously reported elsewhere. The binding energies of the Bi^{3+} 4f7/2 and 4f5/2 core level photoemissions were located at 158.8 and 164.2 eV, respectively. The binding energy locations of the metallic bismuth 4f7/2 and 4f5/2 core level photoemissions were located at 156.4 and 162.2 eV, respectively. These phenomena were attributed to the cleavage of the O–Bi bonds during the Ar

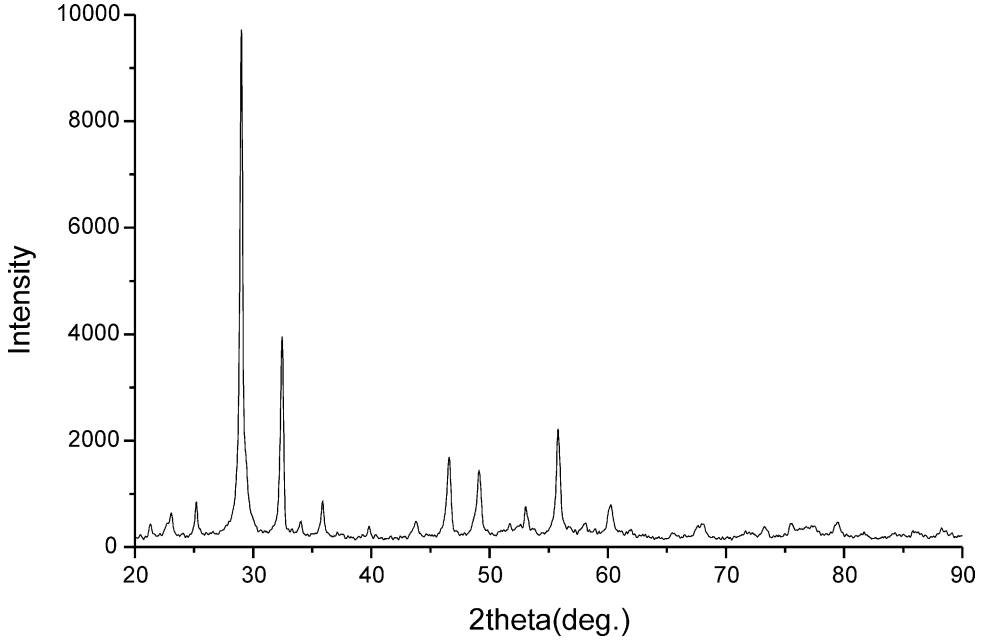

Fig. 7. XRD pattern of the SBT gels calcined at 800 °C for 1 h.

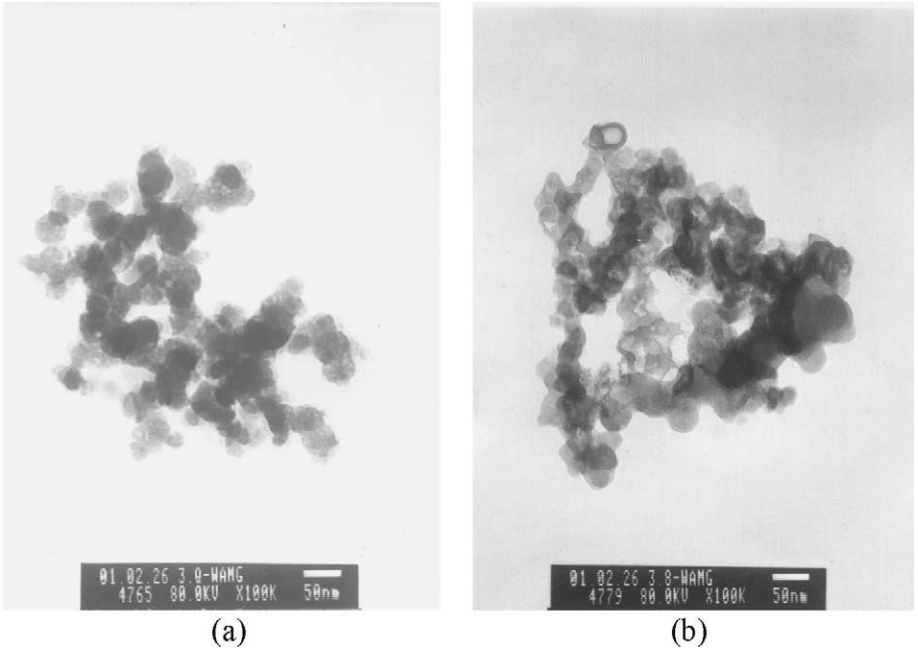

Fig. 8. TEM morphorlogy of the SBT powder (a) gel dried at 100 °C; (b) gel calcined at 800 °C.

ions etching which made bismuth oxide decomposed and reduced to the metallic state.

Figs. 5 and 6 show the XPS signal of valence of tantalum and strontium at the surface and the interface between SBT and platinum. No difference was observed for these spectra of Sr and Ta at the surface and the interface between SBT and platinum. Table 1 lists the binding energies of SBT thin films.

3.3. Structural and morphologic analysis

Fig. 7 shows the XRD pattern of the SBT gel calcined for 1 h at 800 °C, from which the state of phase composites can be determined. The SBT layer-perovskite phase powder obtained has to be single phase.

Fig. 8 shows typical TEM images of SBT dried gel at 100 °C and SBT powders calcined 800 °C, respectively. As shown, the particle sizes are less than 50 nm.

Fig. 9 shows the XRD pattern of a SBT thin film deposited on a $Pt/Ti/SiO_2/Si$ substrate and then annealed at 800 °C for 1 min using RTA. The Pt layer has a predominate (100) orientation, and (115), (200) and other peaks of SBT are seen, indicating that the SBT film has crystallized after being annealed at 800 °C for 1 min.The films prepared by the present technique were single-phase perovskite.

Fig. 10 shows the SEM images of the microstructures of the SBT thin films. The surface of the film is smooth and homogeneous [Fig. 10(a)]. Fig. 10(b) shows the SEM images of the fracture surfaces of the thin film

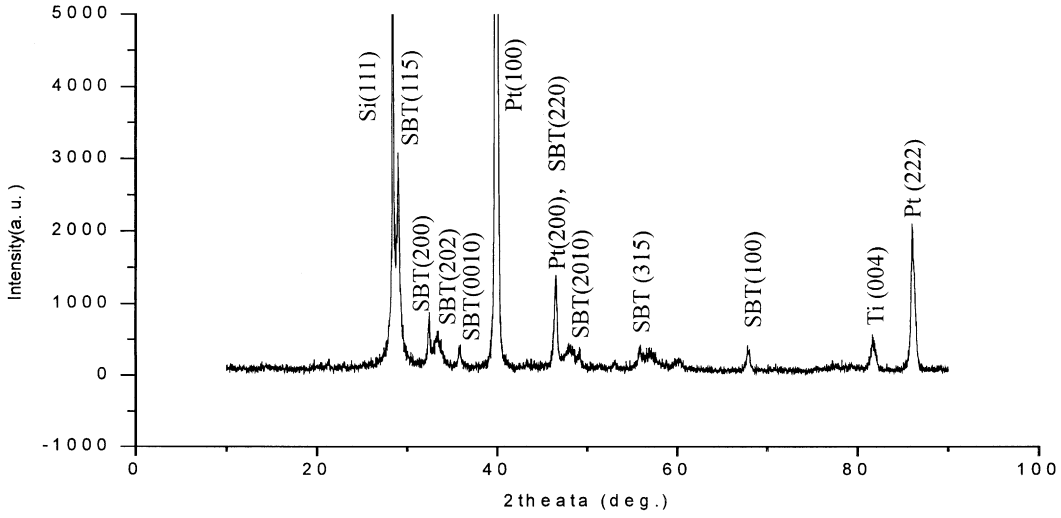

Fig. 9. XRD pattern of the SBT thin films on $Pt/Ti/SiO_2/Si$ substrate.

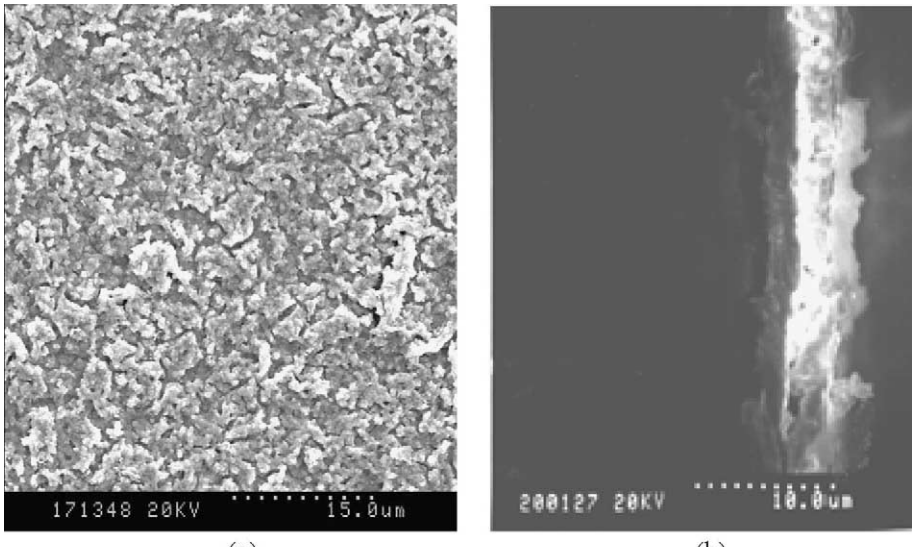

Fig. 10. SEM of the SBT thin films (a) the surface (b) the cross-sectional.

fabricated with ten coating cycles. The thickness of the film is approximately 2 μm and consists of two layers. The upper layer consists of small grains. The composition of the films annealed at 800 °C was about Sr 1.0, Bi 1.8 and Ta 2.0 from measurement by EPMA. When prepared from solution with a mol ratio of strontium: bismuth:tantalum = 1:2:2, the films showed lower Bi content than that of the solution because of vaporization of Bi from the film surface.

Fig. 11a–d shows the morphology and the micro-diffraction (μ-Diffraction) patterns of Pt thin film and the SBT thin film on SBT/Pt/Ti/SiO_2/Si. Fig. 11a and b represent the microstructure and the μ-Diffraction pattern of the film oriented region along [12$\bar{1}$] [Fig. 4(b)],

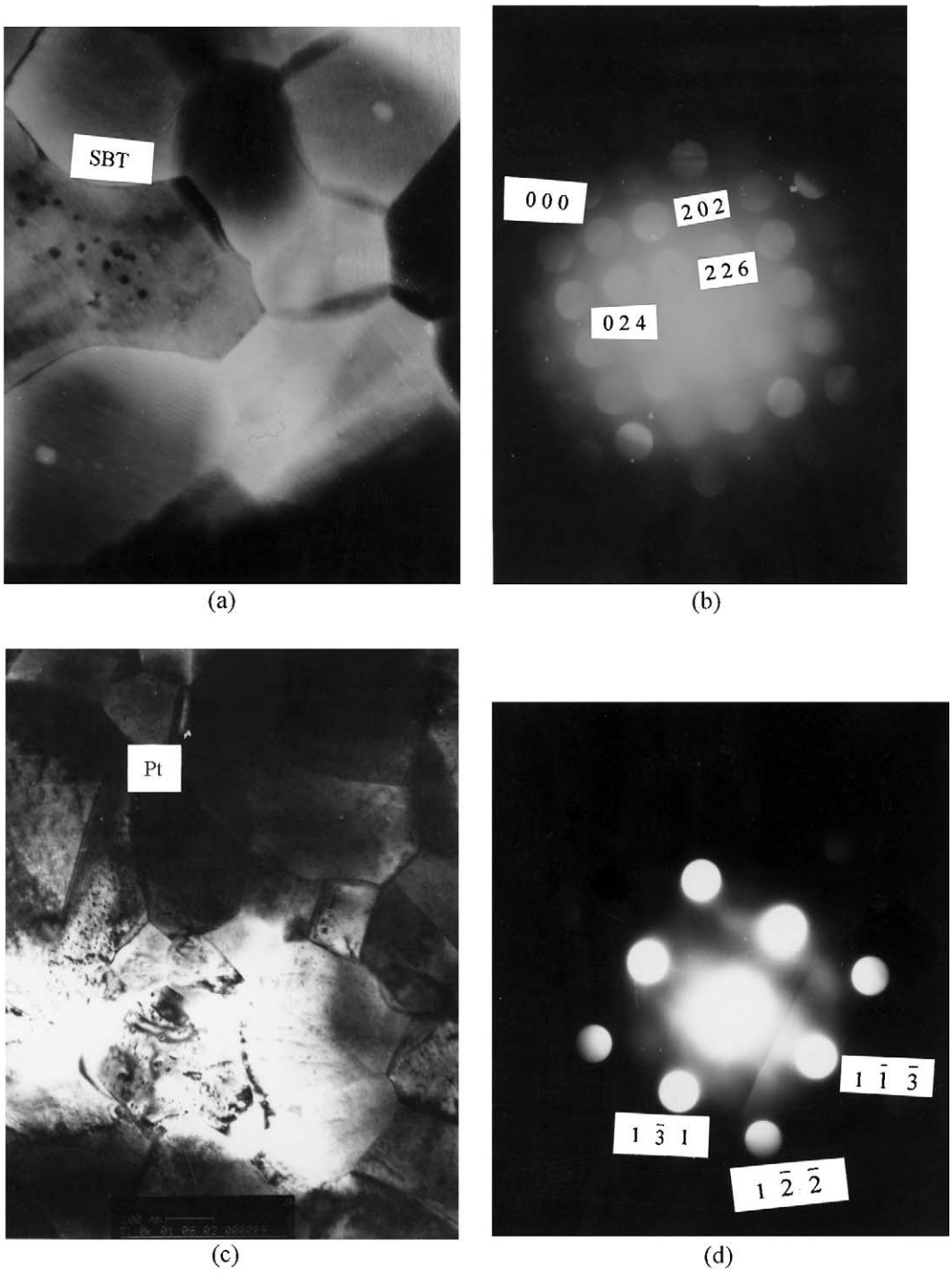

Fig. 11. The morphology and the micro-diffraction (μ-diffraction) patterns of SBT thin film and Pt thin film on SBT/Pt/Ti/SiO_2/Si (a), (b) SBT thin film; (c), (d) Pt thin film.

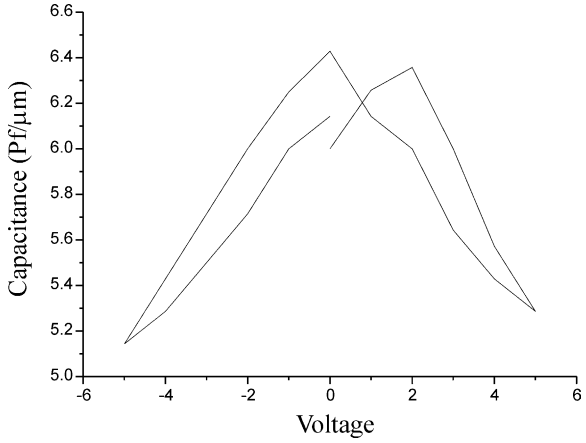

Fig. 12. Capacitance versus voltage (C–V) characteristics of the SBT film.

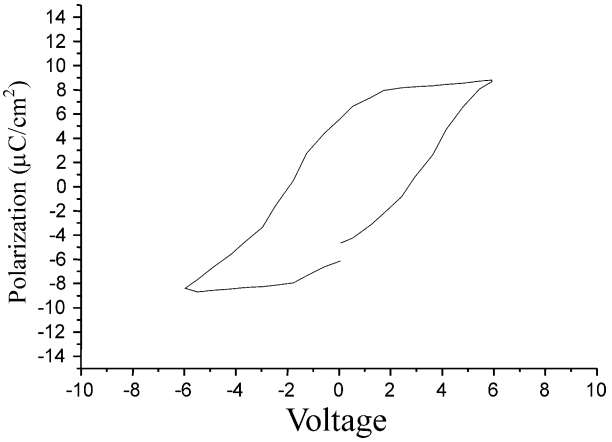

Fig. 13. Hysteresis loops of the SBT thin film.

respectively. The average grain size of the film is about 80 nm.

3.4. Ferroelectric properties

Fig. 12 shows the capacitance versus voltage (C–V) characteristics of 2 μm thick SBT films measured at a frequency 1 MHz. The capacitance was measured when the voltage was swept from a positive to a negative bias and back again.

Fig. 13 shows the hysteresis loop of a 1 μm thick SBT film. A saturated hysteresis loop is observed with a remanent polarization of 5.2 $\mu C/cm^2$, and a saturated polarization of 8.8 $\mu C/cm^2$.

4. Conclusions

A modified sol–gel process is developed to prepare SBT powder and film. Nanocrystalline powder with particle size 50 nm and thin film with thickness 2 μm of $SrBi_2Ta_2O_9$ SBT were successfully prepared by the sol–gel method, using $Sr(Ac)_2{\cdot}1/2H_2O$, $BiONO_3$ and $Ta(OCH_2CH_3)_5$ as source materials, glacial acetic and ethylene glycol as solvents. The SBT layer-perovskite phase powder obtained to be single phase. The Pt layer has a predominate (100) orientation, and (115), (200) of SBT thin film are seen, indicating that the SBT film has crystallized after being annealed at 800 °C for 1 min. The typical hysteresis loop of SBT thin film on Pt/Ti/SiO_2/Si was obtained, and the measured *Pr* and *Ps* value of the SBT thin film were 5.5 $\mu C/cm^2$ and 8.8 $\mu C/cm^2$, respectively.

Acknowledgements

The authors would like to thank Project (HIT.2001.67) supported by the Scientific Research Foundation of Harbin Institute of Technology and Project 50172012 supported by NSFC.

References

[1] D.H. Bao, Z.H. Wang, W. Ren, L.Y. Zhang, X. Yao, Crystallization kinetics of $Ba_{0.8}Sr_{0.2}TiO_3$ sols and sol–gel synthesis of $Ba_{0.8}Sr_{0.2}TiO_3$ thin films, Ceram. Int. 25 (1999) 261–265.
[2] C.A. Araujo, J.D. Cuchiare, L.D. Mcminan, M.C. Scott, J.F. Scott, Fatigue-free ferroelectric capacitors with platinum electrodes, Nature 374 (1995) 627–629.
[3] R. Dat, J.K. Lee, O. Aucielli, A.Z. Kinon, Pulsed laser ablation synthesis and characterization of layered Pt/$SrBi_2Ta_2O_9$/Pt ferroelectric capacitors with practically no polarization fatigue, Appl. Phys. Lett. 67 (4) (1995) 572–574.
[4] T.K. Li, Y.F. Zhu, S.B. Desu, C.H. Peng, M. Nagata, Metalorganic chemical vapor deposition of ferroelectric $SrBi_2Ta_2O_9$thin films, Appl. Phys. Lett. 68 (5) (1996) 616–618.
[5] Z.G. Zhang, J.S. Liu, Y.N. Wang, J.S. Zhu, F. Yan, Fatigue characteristics of $SrBi_2Ta_2O_9$ thin films prepartes by metalorganic decomposition, Appl. Phys. Lett. 73 (6) (1998) 788–790.
[6] Q.F. Zhou, H.L. Chan, C.L. Choy, Synthesis and properties of ferroelectric SrBi2Ta2O9 powder and films prepared by a sol–gel process, J. Non-cryst. Solids 254 (1999) 106–111.
[7] Y. Ito, M. Ushikubo, S. Yokoyama, H. Matsunaga, T. Atsuki, T. Yonezawa, K. Ogi, New low temperature processing of sol–gel $SrBi_2Ta_2O_9$ thin films, Jpn. J. Appl. Phys. 35 (1996) 4925–4929.
[8] D. Ravichandran, K. Yamakawa, A.S. Bhalla, R. Boy, Alkoxide derived $SrBi_2Ta_2O_9$ phase pure powder and thin films, J. Sol–Gel Sci. Technol. 9 (1997) 95–101.
[9] T.J. Boyle, C.D. Buchheit, M.A. Rodriguez, H.N. Shareef, B.A. Hernandez, B. Scott, J.W. Ziller, Formation of $SrBi_2Ta_2O_9$: Part I. Synthesis and characterization of a novel "sol–gel" solution for production of ferroelectric $SrBi_2Ta_2O_9$ thin films, J. Mater. Res. 11 (9) (1996) 2274–2281.
[10] W. Wang, Y. Zhou, S. Chen, F. Ye, D.C. Jia, Preparation of strontium bismuth tantalum (SBT) fine power by sol–gel process using bismuth subnitrate as bismuth source, J. Mater. Sci. Technol. 17 (1) (2001) 25–26.
[11] T. Hayashi, H. Takahashi, T. Hara, Chemical processing and dielectric properties of ferroelectric $SrBi_2Ta_2O_9$ thin films, Jpn. J. Appl. Phys. 35 (1996) 4952–4955.